Evaluating the Type and State of Alaska Taiga Forests with Imaging Radar for Usc in Ecosystem Models

JoBea Way
Eric J. M. Rignot
Kyle C. McDonald
Ram Oren
Ronald Kwok
Gordon Bonan
Myron Craig Dobson
Leslie A. Viereck
Joanna E. Roth

Reprinted from
IEEE TRANSACTIONS ON GEOSCIENCE AND REMOTE SENSING
Vol. 32, No. 2, March 1994

Evaluating the Type and State of Alaska Taiga Forests with Imaging Radar for Use in Ecosystem Models

JoBea Way, *Member, IEEE*, Eric J. M. Rignot, *Member, IEEE*, Kyle C. McDonald, *Member, IEEE*, Ram Oren, Ronald Kwok, Gordon Bonan, Myron Craig Dobson, *Senior Member, IEEE*, Leslie A. Viereck, and Joanna E. Roth

Abstract—**Changes in the seasonal CO_2 flux of the boreal forests may result from increased atmospheric CO_2 concentrations and associated global warming patterns. To monitor this potential change, a combination of information derived from remote sensing data, including forest type and growing season length, and ecophysiological models which predict the CO_2 flux and its seasonal amplitude based on meteorological data, are required. In this paper we address the use of synthetic aperture radar (SAR) to map forest type and monitor canopy and soil freeze/thaw, which define the growing season for conifers, and leaf on/off, which defines the growing season for deciduous species. Aircraft SAR (AIRSAR) data collected in March 1988 during a freeze/thaw event are used to generate species maps and to determine the sensitivity of SAR to canopy freeze/thaw transitions. These data are also used to validate a microwave scattering model which is then used to determine the sensitivity of SAR to leaf on/off transitions and soil freeze/thaw. Finally, a CO_2 flux algorithm is presented which utilizes SAR data and an ecophysiological model to estimate CO_2 flux. CO_2 flux maps are generated, from which areal estimates of CO_2 flux are derived.**

I. Introduction

WITH approximately 21 % of the global soil carbon and 18 % of the global terrestrial live carbon, the boreal forest is the major reservoir of soil organic matter and is second only to broad leaf humid forests in terms of live carbon storage [22]. In addition, uptake and release of CO_2 by the boreal forest may account for approximately 50% of the seasonal amplitude in atmospheric CO_2 at Point Barrow, AK, and about 30% of the seasonal amplitude at Mauna Loa [12]. Based on current estimates of oceanic carbon uptake, Tans *et al.*, [31] Concluded that a northern hemisphere terrestrial carbon sink on the order of 2.0–3.4 Gt C per year is required to balance the global carbon budget. While Tans *et al.* associate this sink with deciduous forests in temperate latitudes, Bonan [7], [8] suggests this sink may actually be a consequence of an imbalance in production and decomposition in boreal forests.

The role of boreal forests in the carbon cycle is particularly important because experiments with atmospheric general circulation models indicate significant northern hemisphere high latitude climatic warming with doubled atmospheric CO_2 concentrations (e. g., [29]). The ecological implications of such a climatic change are unknown, but the seasonal amplitude of atmospheric CO_2 concentrations in northern latitudes has increased with time, and this may reflect increased metabolic activity of ecosystems in northern latitudes due to warmer air temperatures and "CO_2 fertilization" [1], [16], [18]. Change to a warmer, drier climate may release more than 1.75 Gt C per year to the atmosphere from boreal ecosystems [26]. As a comparison, estimates of 1980 annual fossil fuel emission and release of carbon from tropical deforestation are 5.2 Gt C and 0.7–1.4 Gt C, respectively [19]. In addition to increasing metabolic activity, increased high latitude temperatures may also extend the growing season resulting in increased annual productivity, as well as periods of frost drought which may reduce annual productivity.

Based on the above discussion, measurements of the length of the growing season, the length of periods of frost drought, and the seasonal amplitude of CO_2 flux may significantly improve current estimates of net annual CO_2 flux in the boreal regions. Growing season length may be estimated for deciduous species by determining the duration of leaf-on periods. For coniferous species, the summer frost-free period bounds the growing seasonal length. Estimating seasonal amplitude is more difficult. Bonan has developed an ecophysiological model which estimates CO_2 flux based on air temperature, precipitation, relative humidity, air pressure, windspeed, and cloudiness for the dominant species in the Alaskan boreal forests [6], [7]. This model provides a link between parameters which may be remotely sensed (temperature, relative humidity, and cloud cover), and CO_2 flux amplitude which is currently not possible to determine remotely and expensive to es-

Manuscript received April 12, 1991; October 1, 1992; November 2, 1993; revised October 1, 1992; November 2, 1993. This work was carried out at the Jet Propulsion Laboratory, California Institute of Technology, under contract to the National Aeronautics and Space Administration.

J. Way, E. J. M. Rignot, K. C. McDonald, R. Oren, and R. Kwok are with the Jet Propulsion Laboratory, Pasadena, CA 91109.

G. Bonan is with the National Center for Atmospheric Research.

M. C. Dobson is with the University of Michigan.

L. A. Viereck and J. E. Roth are with the Institute of Northern Forestry.

IEEE Log Number 9215454

0190/2802/94$04.00

timate using *in situ* techniques. Applying the model to estimate landscape CO_2 flux requires accurate estimates of the distribution of each forest type.

A number of remote sensing instruments may be used to derive forest type maps and estimate growing season length, and it is likely that a combination of sensors will provide the most accurate information. The Advanced Very High Resolution Radiometer (AVHRR), for example, may provide good estimates of leaf-on period, thus bounding the growing Season length for deciduous spetics. To determine the value of synthetic aperture radar (SAR) for estimating these properties, a series of multitemporal, multifrequency aircraft SAR (AI RSAR) data sets have been collected. These AIRSAR data sets allow us to study the change in microwave backscatter for the seasonal states captured by the AIRSAR and to validate radar scattering models under these select meteorological conditions. The radar models then allow us to determine dominant scattering mechanisms and how they change with the geometric and dielectric makeup of the forest as perturbed by season. The models also allow us to predict forest backscatter at ail frequencies and polarizations over an entire year of hypothetical seasonal states to determine which might be observed by spaceborne SAR systems.

In this paper, wc assess the usc of SAR for mapping boreal forest type and for monitorin g freeze/thaw and leaf on/off transitions. The data set wc usc were collected by the AIRSAR polarimetric aircraft radar over the Bonanza Creek Experimental Forest (BCEF) near Fairbanks, AK, in March 1988 when the trees changed from a thawed 10 a frozen state over a onc-week period. The sensitivity of radar backscatter and scattering mechanism to these changes is demonstrated, as well as our ability to map dominant floodplain forest types using SAR image data. A scattering model validated with the AIRSAR data is then used to determine the sensitivity of SAR to leaf on/off and soil freeze/thaw transitions for which sensor data do not exist. The AIRSAR data arc also used to derive a forest type classification map. Finally, CO_2 flux maps derived from the classification map and an ecophysiological model arc generated for the seasonal states captured by the AIR SAR, and scene average CO_2 flux values arc estimated.

II. Bonanza Creek Experimental Forest Test Site

The test site representing tile Alaskan taiga forest in this study is the Bonanza Creek Experimental Forest (BCEF). BCEF, a Long Term Ecological Research (LTER) site [34], has been the subject of modeling studies by Bonan, Shugart, anti others [2]–[11]. In addition, it is onc of the primary test sites for radar signature studies using the AI RSAR, the European Remote Sensing satellites (ERS-1 anti ERS-2), and the Japanese Earth Resources Satellite (JERS-1) SAR data sets [21], [42].

The 30,000 ha BCEF lies within the Tanana Valley State Forest at latitude 64° 45'N, longitude 148° 15'W in interior Alaska along the Tanana River in the. zone of (discontinuous permafrost. The climate is continental with large diurnal temperature changes, low precipitation, low cloud cover, and low humidity. BCEF includes both upland fire-controlle(i succession and floodplain succession forests. The floodplain fore.sts arc the focus of this paper in order to eliminate topography as a factor in the radar image analysis.

Due to active erosion of mature stands along the Tanana and production of silt bars on the river floodplains, most BCEF forest stands tend to be in a variety of young successional stages [1 5], [36]. Primary succession on the floodplain begins with willows and alder which stabilize the terraces providing biological control of the flooding and allowing the forest floor to develop [36]. Alder (*Alnus tenuifolia*) arc followed by balsam poplar (*Populus balsamifera*) which compete with the shade-intoicmnt alder. Finall y, white spt ucc (*Picea glauca*) dominate on river alluvium where permafrost is absent. In locations where the white spruce stands arc protected from erosion, their shading allows the formation of permafrost, which then results in a final successional transition to black spruce (*Picea mariana*).

III. Canpoy Freeze/Tl iaw Observat ions with AI RSAR

Freezing and thawing of the soil and trees define the limits of the growing season anti the duration of frost drought for the coniferous forests. Preliminary observations with airborne SAR indicate a clear ability to monitor canopy freeze/thaw events [42]. A quant itat ive assessment of these observations is presented along with *in situ* data and microwave modeling results, which arc used to explain the interaction of the radar with the forests under different meteorological conditions.

A. Observations

A it borne SAR data collected with the Jet Propulsion Laboratory's (JPL's) P-, 1.-, and C-band (0.450, 1.26, and 5.31 GHz, respectively) polarimetric AIRSAR mounted in NASA's DC-8 aircraft were acquired over the BCEF test site on five flight days in March 1988 [42]. Overlapping passes were acquired on March 13, 17, and 19. Data collected on March 11 and 21 were offset by approximately a half-swath-width and will not be used due to incidence angle differences. On March 17, the P-band radar lost its V-transmit capability; anti on March 13, turbulence in the air resulted in banding in the C-band data. Data collected on March 17 and 19 arc nearly identical in backscatter because air temperatures were well below freezing on both days. The March 13 data were collected during an unusually warm period (temperatures were above 0°C) and show significantly higher backscatter than the two colder days. 'J'able I summarizes the AIRSAR data sets for March 13, 17, and 19. Given the above considerations, wc will focus on the L-band data collected on March 13 anti 19.

TABLE I
AIRSAR PARAMETERS AND ENVIRONMENTAL CONDITIONS AT TIME SOIL OVERFLIGHTS

Date		3/13/88	3/17/88	3)19/88
Local time of overflight		15:03	14:54	23:17
AIRSAR channels		P, L*	L, C**	L, C**
Incidence angle***		41°	40°	39°
Maximum air temperature	(C)†	10	-12	-8
Minimum air temperature	(C)†	-13	-19	-17
At Time of Overflight:				
Air temperature(C)		2	-13	-14
Soil temperature				
5 cm depth	' ("	-2	-3	-3
50 cm depth		0	-1	-1
Snow temperature (C)		0	-13 1	-12
Snow upper layer	condition	wet	frozen	frozen
Snow moisture (%	vol)	S.-i	0	0
Stem water status		thawed	frozen	frozen

* Rain during C-band data due to air turbulence
** H-pol transmit channel only for P-band
*** At center of Seven Mile Island
† From LTER 2 on flood plain

The March 13 and 19 L-band data were calibrated radiometrically to + /-- 1.9 dB using 6′ corner reflectors [21], and color density slice total power images were generated (Fig. 1). The red regions along the Tanana River in the March 13 image represent the mature stands of white spruce and balsam poplar frond on the floodplain, while the blue regions in this image represent stands of black spruce. The region to the south of the Tanana River is black spruce and bog. In the March 19 L-band scene, white spruce and balsam poplar backscatter are reduced by about 5-7 dB resulting in blue-colored stands with our color scheme. The image was collected from the south; stands along the north bank of the river in the March 19 scene remain bright (red) due to a stem-river corner reflector return.

B. Analysis

In order to understand the causes for the change in backscatter with freezing and thawing, radar scattering models are employed. *In situ* data, including both static (geometry and species) and temporally varying canopy properties collected at the time of overflight, are used as input to radar scattering models to determine the expected backscatter from the forest, and the results are compared to the measured backscatter signatures (Fig. 2). Agreement for a variety of frequencies, polarizations, and seasonal states indicates the radar scattering through the canopy is correctly modeled. By then looking at the various contributions to the total backscatter as identified in the model, insight into the dominant scatterers can be ascertained.

1) In Situ Data: In situ data collection includes static canopy and soil properties, including species, stem diameter and height, and canopy dimensions, and temporally varying properties which must be acquired at the time of SAR data collection. Temporally varying properties include canopy water status and dielectric properties, and snow moisture properties. The complete set of measured canopy properties is documented on a CD Rom by Way et al. [45].

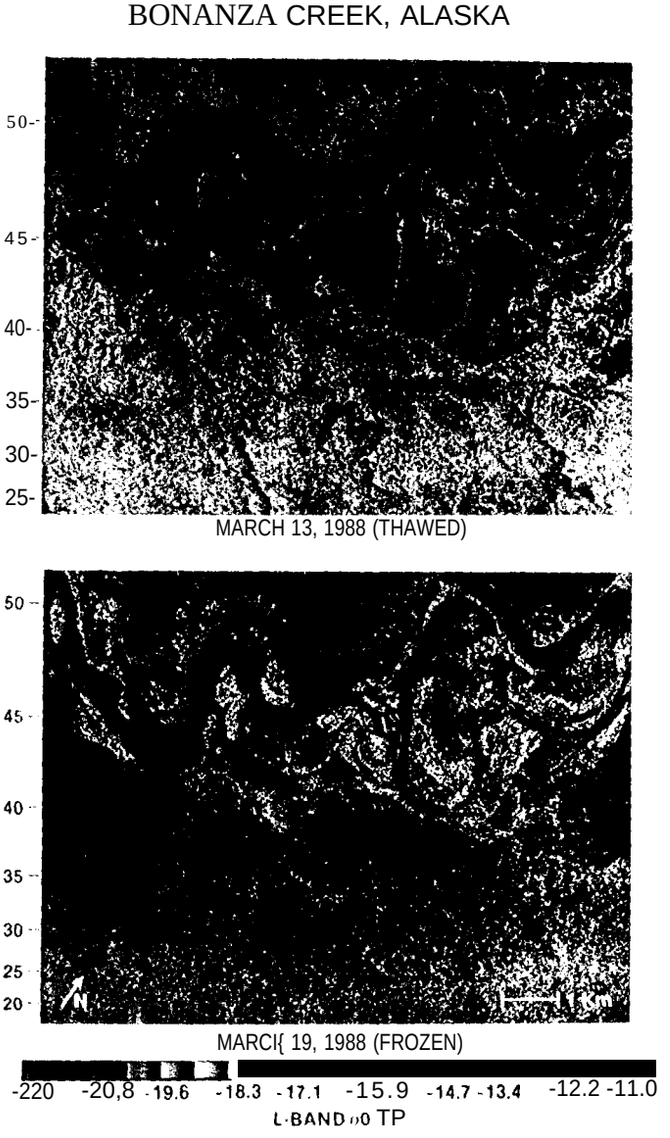

Fig. 1. Calibrated total power backscatter image of BOREAS on March 13 (thawed) and March 19 (frozen). The red areas in the March 13 image are white spruce and balsam poplar. In general, the blue areas are black spruce and clearcuts. The Tanana river runs approximately east-west through the image.

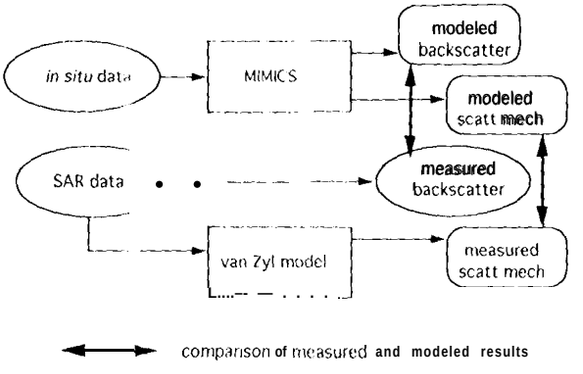

Fig. 2. Modeling pathways showing the use of MIMICS and the van Zyl model to understand the interactions of the radar with the forests.

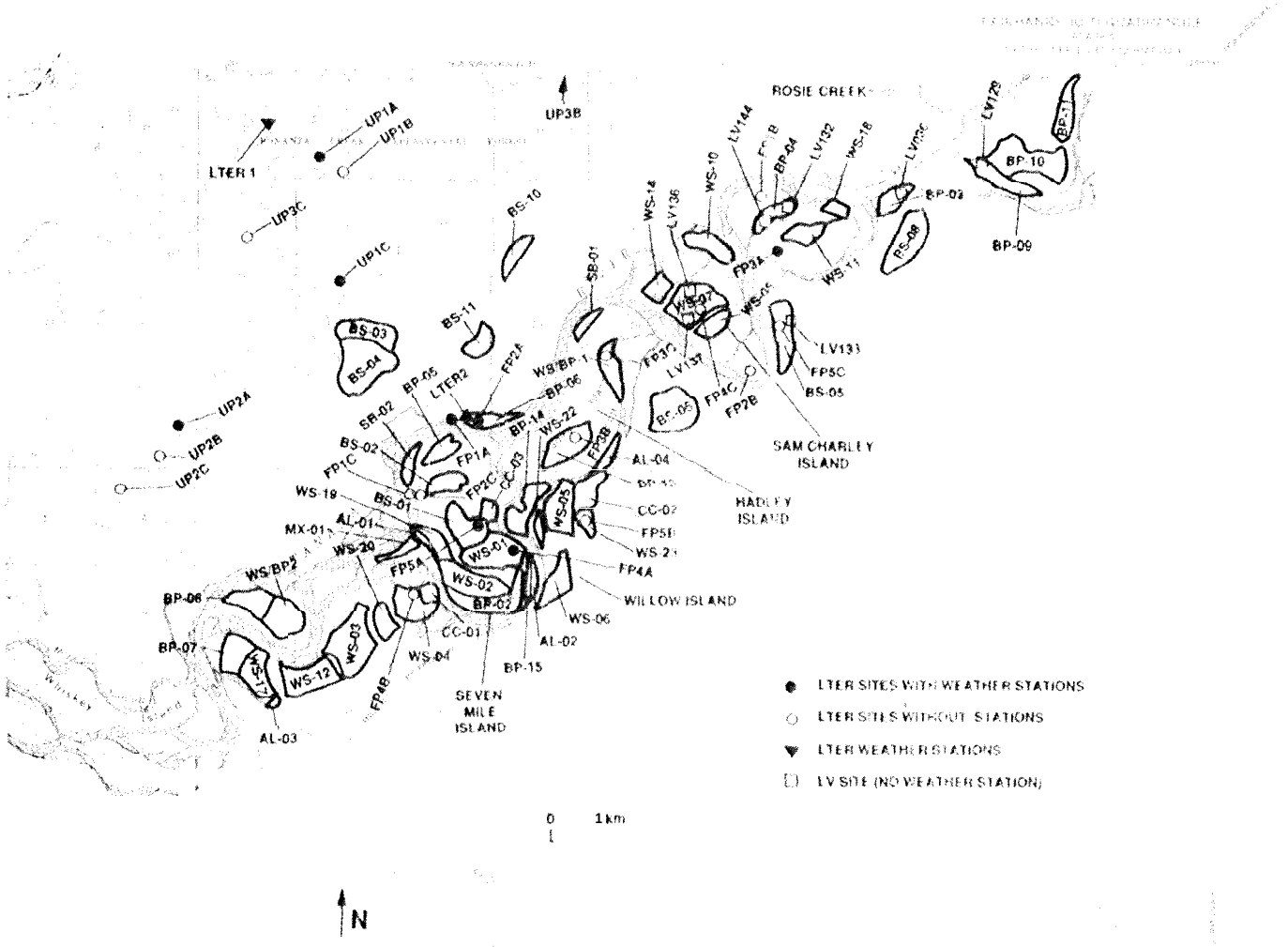

Fig. 3. Bonanza Creek Experimental Forest (BCEF) showing test stands used in this study. Also shown are the LTER weather stations.

a) Static Canopy Geometry: Approximately 30 forest stands (including 3 clear-cuts) in BCEF have beenidentified for this study (Fig. 3). 'T'0 date, canopy geometric characteristics have been collected for 12 stands (Table 11): 5 were obtained during the March AIRSAR experiment and in the summer of 1988 [20], and 7 additional stands have been measured in the summer of 1990 [28].

Each standconsists of 10 measured plots separated by 50-100 m and distributed along one or two transects through the stand. Approximately 150 trees pcr stand were measured for stem diameter at breast height (DBH) and number density, where a tree is definedas having aDBH of at least 2.5 cm. Forty trees (approximately four pcr plot) of each species frequent in the overstory were selected for height measurements. From the DBH and height data, linear regressions relating DBH and height were used to estimate heights for all trees in the measured plots. Biomass was calculated using equations by Yarie and Van Cleve [47], Manning *et al.* [23], and Singh [30]. The mean of height, DBH, stem number density, percent canopy cover, and winter biomass for each stand are summarized in Table 11.

For balsam poplar, the mean heights for the mature stands arc 15- 17 m with mean DBH's of 18 cm and a stcm density of 1125-1615 stems/ha. The younger balsam poplar stand has a much smaller DBH and height and a much largei stem density as is typical of young stands. The white spruce stands are similar in height and DBH to the balsam poplar stands with mean heights ranging from 20 to 22 m, mean DBH's ranging from 14 to 25 ctn, ant] stem densities from 608 to 2073 stems/ha. The black spruce stand is quite different in diameter and height with mean heights from 7 to12 m and mean DBH's of 8-13 cm. The stem density is similar at 1135- 1975 stems/ha.

b) Temporally Varying Canopy Properties: During the aircraft overflights, several scene variables (stem water status and dielectric characteristics, and snow pack characteristics, including moisture and temperature) were obtained on Seven M ile Island in the WS-02 and 11S-01 stands. Air temperature and relative humidity were mon-

TABLE II
MEASURED CANOPY PARAME II RS

Stand	Location	Age (years)	Mean DBH (cm)	Mean Height (m)	Density of Live Stems (#/ha)	Canopy Cover (%)	Winter* Biomass (10^3 kg/ha)
Clearcuts							
CC-1	Sev en Mile Isl	6 (1985/6)	0	0	0		0
CC-2	Willow Isl	Y (198? /3)	0	0	0		0
Alder (*Alnus tenuifolia*)							
AL-1	Seven Mile Isl	30	50	6.9	790,	86	21 (29)
Balsam Poplar (*Populus balsamifera*)							
BP-2	Seven Mile Isl	9[]	18.0	17.6	1615		179 (182)
BP 6	Davis Trail	30	7.3	9.1	3699	71	34 (M)
BP-13	Hadley [']I	75 est	18.5	15.2	1125	45	104 (106)
White Spruce/Balsam Poplar							
WS/BP-1	Hadley Isl	50	9.3	10.4	4997	5(1	109(11[])
White Spruce (*Picea glauca*)							
WS 1	Seven Mile Isl	165	19,6	22 1	1248		217
WS ?	Seven Mile Isl	)00	145	201	2073		167
WS 4	Seven Mile Slough	124	25.0	2211	608	49	163
WS 5	Willow Isl	180	17.9	21 3	1486		181
Black Spruce (*Picea mariana*)							
BS 1	Seven Mile Isl	200	8.8	7.6	1975		37
BS-2	Sev en Mile Isl	2[10	8.2	6.8	1402	14	23
BS 12	Willow Isl	2[1[1	13.9	12.3	1135	29	60

* Summer biomass noted in () for alder and balsam poplar
** In or adjacent to LTER stands

itored hourly using two LTER weather slat ions located in the uplands (LTER- 1) and on the floodplain (1 TER-2) (see Fig. 3). in addition, soil temperatures at 5, 10, 20, anti 50 cm depths at the two LTER weather stations were recorded throughout the duration of the flights. These temporally varying measurements are discussed in detail by Way *et al.* [42] and are summarized in '1'able 1.

Throughout the experiment between March 11 and 21, the Tanana River remained frozen and there was approximately 20-25 cm o{ snow on the ground. No deciduous trees (balsam poplar and aspen on the floodplain and birch and alder in the uplands) had leaves. The average air temperature dropped from 2°C on March 13 to -- 14°C on March 17 and 19. Soil temperatures remained at () to −3°C on all three days. Snow temperature was 0°C on March 13, and the upper layer was wet during AIRSAR data acquisition: while on March 17 and 19, the snow temperat u re d ropped to 13°C, and the snow was frozen throughout. On the warm day, snow moisture rose to 5-7% on March 13 but dropped to 0% on March 17-19.

One of the canopy characteristics which strongly affects the radar signature is the dielectric constant. Although it was not possible to determine the dielectric constant for the entire tree, measurements of the stems were obtained using a field-portable Applied Microwave dielectric probe and a O. 141 "-diameter tree tip. Data were collected at several depths in the white and black spruce and balsam poplar on each of the {light days. The results are shown in Fig. 4. For white spruce on the thawed day, the real dielectric constant reaches a peak of about 35 at about 3 cm depth. At greater depths, the dielectric constant decreases rapidly and reaches a constant value at about 6 cm depth. in comparing the measured dielectric constant profiles to tree core profiles, the higher dielectric constant region corresponds to the xylem tissue with the highest hydraulic activity. Balsam poplar shows a similar pattern.

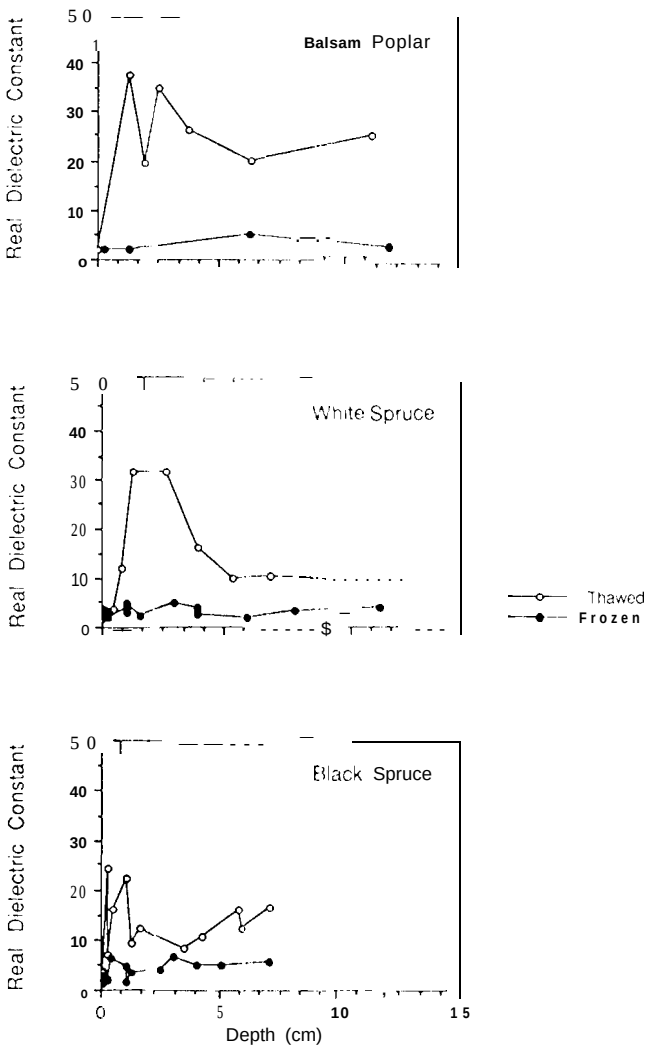

Fig. 4. L-band real dielectric constant versus depth into the stem for balsam poplar, white spruce, and black spruce for the frozen and thawed days in March 1988.

The black spruce has a more uniform dielectric profile on the thawed day, reaching a peak of about 25 between about 1 and 2 cm depth. On the frozen day, the real dielectric constant profiles for both trees show a dramatic drop to below a dielectric constant of 5 at all depths due to freezing of the xylem liquids. The higher dielectric constants in the active xylem region of the thawed trees are due to the freely rotating polar water molecules. Upon freezing, rotation is halted and the dielectric constant drops significantly.

2) Backscatter Signature Extraction: The measured L-band backscatter for the frozen and thawed days for the 12 stands and two clearcuts are plotted as a function of age and species in Fig. 5 for all three polarizations (HH, VV, and HV). The difference due to freezing is large at all three polarizations for all three stands, with the greatest difference at vertical and cross polarizations.

Table III shows the mean and standard deviation for the measured backscatter values for the balsam poplar, white spruce, and black spruce stands. Table IV summarizes the results of a two-way analysis of variance with a least squares difference (LSD) at the 0.05 significance level. These results indicate that there is an interaction between species and freeze/thaw state for LVV (i.e., the relationship between the frozen and thawed backscatter changes with species, and the significance of the interaction is <0.05); however, for LHH and LHV, there is no interaction between species and freeze/thaw state (significance of interaction is >0.05). For LHH and LHV, then, the backscatter from the black spruce is significantly different from white spruce and balsam poplar, but the backscatter from white spruce and balsam poplar are not significantly different at either polarization.

3) Microwave Modeling: To gain insight into the cause for the change in backscatter between the frozen and thawed states, radar scattering models may be employed. In our analysis, we use the Michigan Microwave Canopy Scattering (MIMICS) model.

a) The MIMICS Model: The MIMICS model is a fully polarimetric first-order radiative transfer model developed at The University of Michigan specifically for modeling radar backscatter from tree canopies. The version of MIMICS applied in this study (MIMICS 1) has been developed for application to canopies with continuous or nearly continuous crown layers. This section provides a very brief introduction to **MIMICS** 1. The complete derivation of the model is quite lengthy, and therefore the reader who desires more information about the derivation of the radiative transfer solution is referred to [32] or [33].

As confirmed in a number of modeling studies [ ] 3], [14], [24], [25], MIMICS is valid for microwave frequencies between P- and X-bands, multiple polarizations, and over a wide range of incidence angles. In these analyses, extensive sets of canopy data derived from *in situ* ground measurements were used as input to MIMICS, and the resulting model output was compared to multipolarization radar data recorded with truck-mounted scatterometers and aircraft-mounted SAR's. Results of these studies have given confidence in the performance of MIMICS.

MIMICS models a forest canopy as two distinct horizontal vegetation layers comprised of the tree crowns and stems (or trunks) over a dielectric ground surface. The incident-specific intensity is related to the scattered intensity through a transformation matrix found by applying

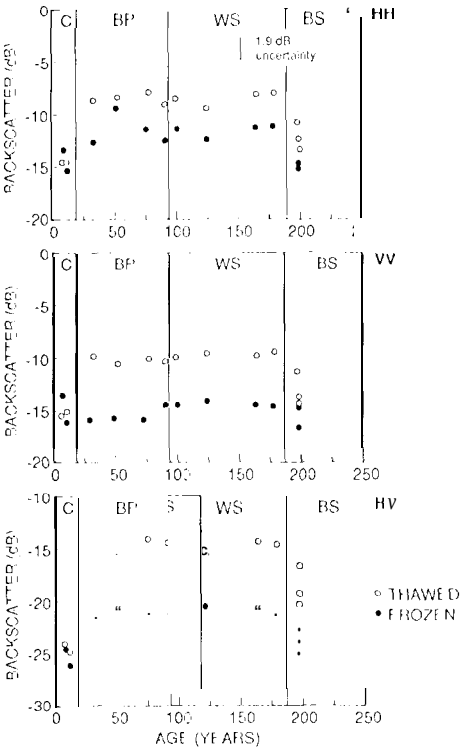

Fig. 5. Extracted backscatter signatures from the calibrated AIRSAR images for the frozen and the thawed days plotted as a function of age for the clearcuts, balsam poplar, white spruce, and black spruce. Note that the backscatter on the thawed days is always higher than on the frozen days at L-band.

TABLE III
MEAN MEASURED L-BAND BACKSCATTER AND STANDARD DEVIATION

Species	LVV (dB) Frozen	LVV (dB) Thawed	LHH (dB) Frozen	LHH (dB) Thawed	LHV (dB) Frozen	LHV (dB) Thawed
BP	-15.5 (0.8)	-10.0 (0.2)	-12.2 (0.7)	- 8.5 (0.5)	-21.2 (0.2)	-13.8 (.2)
WS	-14.5 (0.3)	- 9.4 (0.3)	-11.5 (0.5)	- 8.4 (0.6)	-20.7 (0.3)	-14.1 (.3)
BS	-16.1 (1.0)	-13.2 (2.0)	-14.4 (0.9)	-12.1 (1.4)	-23.7 (1.2)	-18.6 (1.9)

TABLE IV
RESULTS OF TWO WAY ANALYSIS OF VARIANCE

Freq/Pol	Variable	Deg. of Freedom	F	Significance*
LVV	Species	3	16.2	<.001
	State	2	127.3	<.001
	Interaction	1	3.76	.049 (yes)
LHH	Species	3	331	<.001
	State	2	722	<.001
	Interaction	1	122	.374 (no)
LHV	Species	3	37.8	<.001
	State	2	265.6	<.001
	Interaction	1	2.6	.113 (no)

* significance level is 0.05

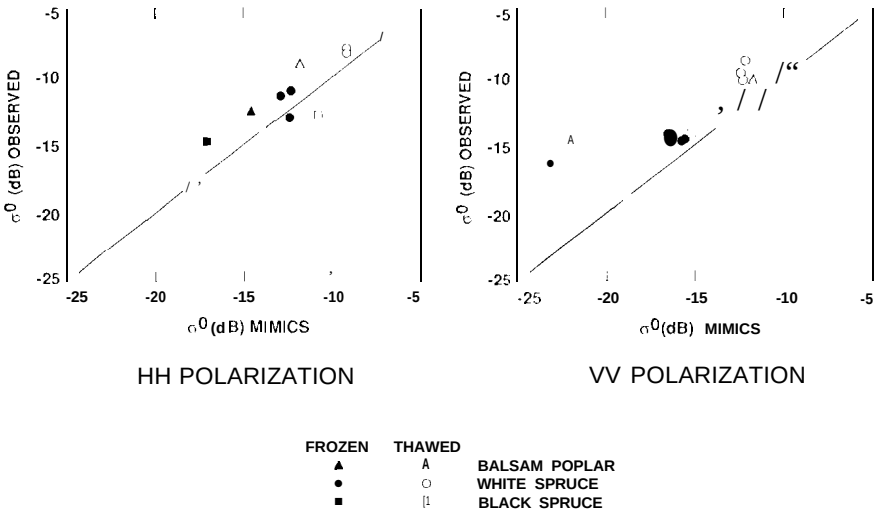

Fig. 6. L-band backscatter as estimated using the MIMICS model and extracted from AIRSAR data for both the thawed (March 13) and the frozen (March 19) days for balsam poplar (a), white spruce (b), and black spruce (c). }1}1, VV, and HV results are shown.

radiative transfer equations in the crown and stem layers, applying boundary conditions at the ground surface and vegetation boundaries, and using an iterative technique to solve for canopy backscatter.

Two classes of parameters are relevant for model development. These are 1) the dielectric parameters that specify the electrical properties of canopy constituents, and 2) the geometric parameters that specify the shapes, sizes, and spatial distribution 01 the canopy constituents, Dielectric constants may be used directly as input to the model, or may be inferred from the appropriate constituent parameters. in this study, dielectric parameters have been inferred using the *in situ* measurements acquired during the experiment and through applications of various dielectric models [13], [14].

Dielectric cylinders are used to model stems, branches, and needles, while disks are used to model leaves. The size and orientation of each class of vegetation constituent is defined in terms of a probability density function (PDF). In general, the crown layer consists of constituent classes such as branches, leaves, or needles, each with a corresponding number density of particles per unit volume. The geometric parameters applied in this study have been inferred through sets of *in situ* measurements and through application of allometric equations [13], [14].

b) MIMICS Validation with AIRSAR Data: The measured ground and canopy characteristics described above were used to validate the MIMICS scattering model. Dobson *et al.* [14] discuss this validation in detail. The results are shown in Fig. 6. In summary, the measured and modeled backscatter values match within 1 till for all canopies and freeze/thaw states except when the ground interaction is significant. The mismatch is primarily due to modeling the snow-covered surface as a single half-space as opposed to a half-space covered by a snow layer.

Fig. 7 summarizes the scattering interactions at L-band.

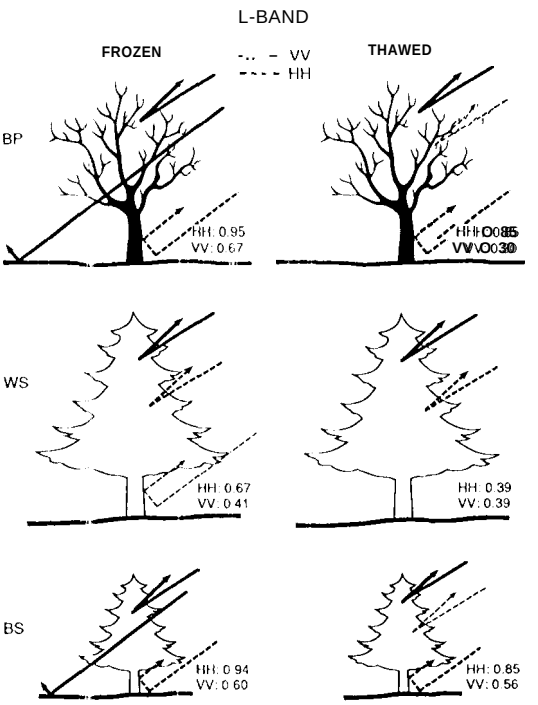

Fig. 7. Dominant interactions for L-band scattering from balsam poplar, white spruce, and black spruce on both the frozen and the thawed days. HH (dashed line) and VV (solid line) interaction are shown if the backscatter return is significant. At the lower right of each figure, the ratios of stem-ground to total backscatter for HH and VV are shown.

Numbers to the lower right for each case are the ratio of stem-ground to total backscatter for HH and VV.

The total backscatter from frozen balsam poplar is small; most of the energy passes through the canopy and is scattered in the forward direction or is attenuated by the ground as the low dielectric properties of the trees do not contribute significantly to the backscatter. There is a small amount of scattering, however, from both the direct crown

(primarily VV) and the stem-ground (primarily HH). When the balsam poplars thaw, both VV and HH scattering from the crown increase, although the HH term is still dominated by stem-ground. HV backscatter from diffuse canopy scattering also increases significantly between frozen and the thawed states due to the increased dielectric constant of the canopy [14].

For white spruce, VV scattering is dominated by crown scattering for both the frozen and the thawed conditions. For the frozen condition, HH scattering includes stem-ground and crown scattering; white for tbc thawed condition, HH scattering is primarily from the crown. As with the balsam poplar, the HV backscatter increases significantly with thawing due to the increase in canopy dielectric constant [14].

For black spruce, as with balsam poplar, there is little backscatter return in the frozen condition; however, the HH return is dominated by stem-ground scattering, and the VV return by direct crown return. When the black spruce thaws, VV scattering is primarily from the direct crown, while HH scattering is from both the direct crown and stem-ground. in general, for L-band imaging of the forests under frozen conditions, the canopy tends to show limited interaction with tile radar signals, while for the thawed canopy, there is scattering from both the stem and the canopy. VV scattering is dominated by crown returns in both the frozen and the thawed conditions, while HH scattering has a significant stem-ground component in both the frozen and the thawed states.

c) *van Zyl Model:* The van Zyl model [39] uses polarimetric SAR data for unsupervised classification of the scattering behavior by comparing the polarization properties of each pixel in an image to that of simple classes of scattering such as even number of reflections, odd number of reflections, and diffuse scattering. The following criteria determine the dominant scattering mechanism:

specular if:

$$\mathrm{Re}(HH\ VV^*) > HV \quad \text{(pixels colored blue)}$$

corner reflector if:

$$-\mathrm{Re}(HH\ VV^*) > HV \quad \text{(pixels colored red)}$$

diffuse if:

$$|\mathrm{Re}(HH\ VV^*)| < HV \quad \text{(pixels colored green)}.$$

Results using the van Zyl model arc presented by Kwok *et al.* (this issue) for the frozen and thaweddays.

As both the MIMICS model and the van Zyl results indicate, the dominant L-band scattering for thawed forest is from the canopy and is diffuse for both white spruce and balsam poplar. Both MIMIC'S and van Zyl's model indicate single bounce scattering from tile canopy for frozen white spruce. For frozen balsam poplar and black spruce, the MIMIC'S model predicts significant stem-ground return, while the van Zyl model shows primarily specular scatter from the crown.

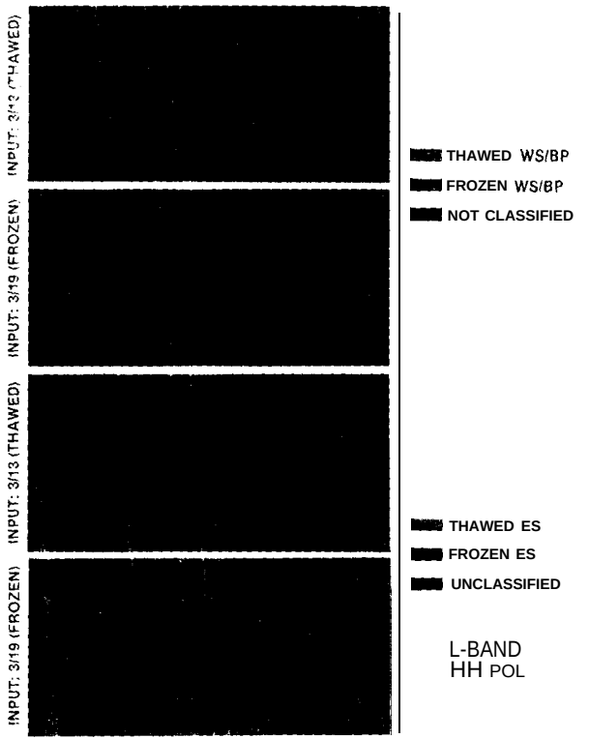

Fig. 8. Classified images for the thawed (red) and frozen (blue) white spruce/balsam poplar. The input was the March 13 (a) and March 19 (b) AIRSAR data. Classified images for the thawed (red) and frozen (blue) black spruce. The input was the March 13 (c) and March 19(d) AIRSAR data. Black indicates the backscatter is outside the specified classification range.

c. *Regional Monitoring*

The above results indicate that it is possible to determine canopy freeze/thaw state in Alaskan forests based on the analysis of a few select stands in BCEF. Our ability to estimate freeze-thaw state on a regional basis may be addressed by analyzing the entire AIRSAR scene.

A simple backscatter level slicing routine was used to classify frozen and thawed forests in the Bonanza Creek scene. Using the March 1988 L-band HH results for the measured test stands, the following classification units could be identified for white spruce/baisiill~ poplar (WS/BP) as a single forest unit:

$$-9.8\ \mathrm{dB} < \sigma_0 < -7.5\ \mathrm{dB} \quad \text{thawed WS/BP} \quad (1)$$

$$13.5\ \mathrm{dB} < \sigma_0 < 9.8\ \mathrm{dB} \quad \text{frozen WS/BP} \quad (2)$$

and for black spruce (BS) as a single unit:

$$-13.7\ \mathrm{dB} < \sigma_0 < -10.7\ \mathrm{dB} \quad \text{thawed BS} \quad (3)$$

$$-15.1\ \mathrm{dB} < \sigma_0 < -13.7\ \mathrm{dB} \quad \text{frozen BS.} \quad (4)$$

Note that frozen WS/BP and thawed BS have similar backscatter signatures.

The classification results are shown in Fig. 8. Thawed

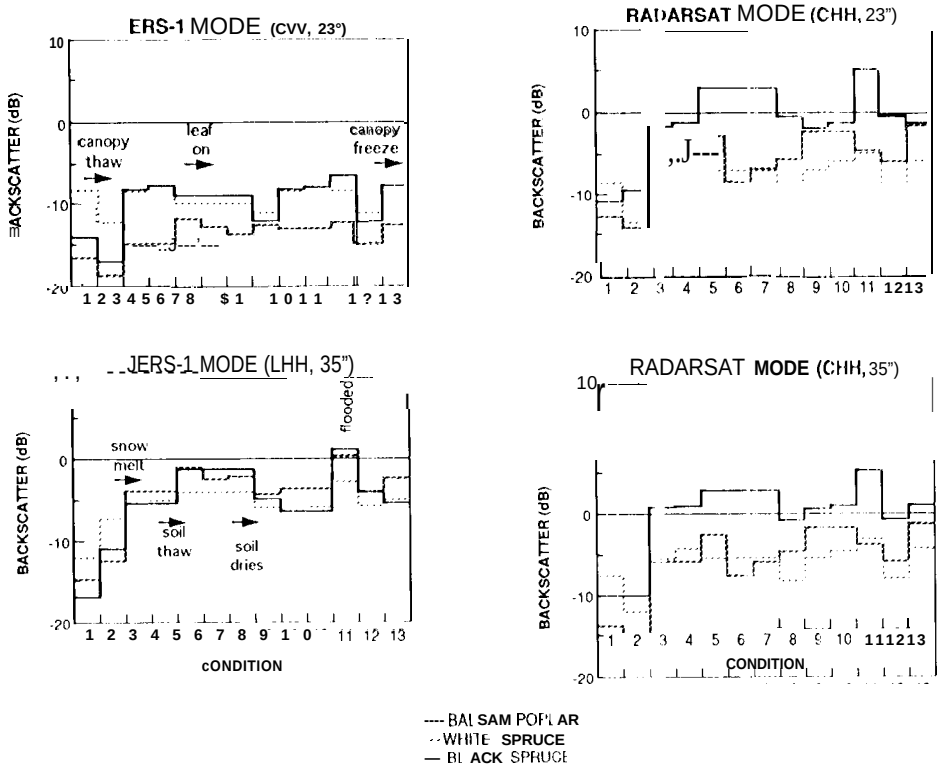

Fig. 9. Seasonal backscatter simulations derived using the MIMICS model for ERS-1 (a), JERS-1 (b), and RADARSAT at 23° (c) and 35° (d) incidence angles.

stands are colored red, frozen stands are colored blue, and stands outside the classification limits are black. in Fig. 8(a) and (b), frozen and thawed WS/BP stands are identified using the original AIRSAR data as input and equations (1) and (2). On March 13 [Fig. 8(a)], thawed WS/BP stands are correctly identified (colored red); thawed BS stands are mistaken for frozen WS/BP stands and colored blue. On March 19 [Fig. 8(b)], all WS/BP stands are correctly identified as frozen (colored blue); most BS stands are outside the limits specified for frozen or thawed WS/BP and are colored black. The misclassification of trees along the river as thawed WS/BP occurred because the stem - ground interaction of the Molar with border trees occurs without attenuation through the canopies of' neighboring trees, resulting in a greater return than from the rest of the stand.

In Fig. 8(c) and (d), frozen and thawed BS are identified using equations (3) and (4). On March 13 [Fig. 9(c)], thawed BS stands are correctly identified. '1'hawed WS/BS stands are outside the limits set for frozen and thawed BS and are colored black. On March 19 [Fig. 8(d)], frozen BS stands are correctly colored blue, however, WS/BP stands are identified as thawed BS and colored red.

in addition to using backscatter as an indicator of freezing, scattering mechanism may be used for white spruce anti balsam poplar. For both spccics, a change from specular to diffuse scatter indicates a change from frozen to thawed canopy conditions.

IV. Soil Freeze/Thaw and Deciduous Leaf On/Off Model Simulations

No data exist for which the soil thaws or tile leaves come out or fall; therefore, we will use the MIMICS model which has been validated for the available canopy freeze/thaw conditions to simulate expected soii freeze/thaw and leaf on/off backscatter signatures. Wc focus on L-band HH and C-band VV and HH SAR channels as these are the ones that will be available with current and future spaceborne SAR missions, including ERS-1 and ERS-2, JERS-1, and RADARSAT. Also included are simulations for canopy freeze/thaw such that C-band changes may be addressed.

The model within MIMICS for scatter from snow-covered ground was developed and validated for application at 1.-hand. As this model may not necessarily be applicable at C-band, some ambiguities may result in the C-band model simulations with respect to changing snow conditions.

A. Model Simulations

The seasonal cycle in the soil-tree system for each of the primary floodplain forest types may be arbitrarily divided into several stages which should correspond to distinct signatures in the SAR data; these are shown in '1'able V. The conditions include canopy free/c/thaw (condition 1-2), snow melt (2-3), drying of spruce needles under frost drought (3-4), soil thaw accompanied by an increase in needle moisture and water potential (4-5), leaf-on for the

TABLE V
SPECIFIED ENVIRONMENTAL AND PHENOLOGIC CONDITIONS FOR MIMICS SIMULATION MODELING

Condition	Environment			Balsam Poplar			Spruce		
	Air Temp	Soil state	Snow State	Water Content State/Potential Leaves	Stem		Water Content State/Potential Needles	Stem	
1	<0°	frozen	dry		frozen	0	frozen	frozen	0
2	>0°	frozen	Wet		normal	0	normal	normal	0
3	>0°	froz	en		normal	0	normal	normal	d)
4	>0°	frozen			normal	0	dry	dry	<0
5	>0°	moist		-	normal	u	normal	normal	0
6	>0°	moist		high	normal	0	normal	normal	0
7	>0°	moist		normal	normal	0	normal	normal	0
8	>0°	dry		normal	normal	<0	normal	normal	0
9	>0°	dry		dry	dry	<0	normal	normal	<0
10	>0°	dry		dry	dry	d)	dry	dry	<0
11	>0°	flooded		normal	normal	0	normal	normal	0
12	<0°	frozen			norms)	0	normal	normal	0
13	<0°	frozen			frozen	0	frozen	frozen	0

Note: Condition 1 is the same on March 13, 1988; and condition 2 is the same as March 17 and 19 1988

balsam poplar (5-6), a summer decrease in leaf moisture (6-7), drying of the soil and stressing of the balsam poplar (7-8), drying of the balsam poplar leaves (8-9), drying of the spruce needles (9- 10), flooding (1 0- 11), soil freezing and leaf fall (11-12), and canopy freezing (12-13). The difference between conditions 1 and 13 is due to snow.

1) ERS-1 Parameters: Backscatter as a function of seasonal state was simulated using ERS-1 radar parameters (C-band, VV polarization, 23° incidence angle) for the conditions shown in Table V. ERS-1 was launched in July 1991 and will be in orbit nominally through 1994. ERS-2 will follow ERS-1 with a launch in the 1994/5 timeframe. Table VI summarizes the soil and canopy properties used in the simulations. The simulation results are shown in Table VII and Fig. 9(a).

For C-band VV for all three forest types, there are large total changes in the backscatter over the year of 6.8 dB for balsam poplar, 4.3 dB for white spruce, and 10.6 dB for black spruce. All three forest types show a drop in backscatter when the stem and snow are thawed relative to frozen. All three canopies also show an increase in backscatter between conditions 2 and 3 when the wet snow disappears and the spruce become stressed. Soil thawing (condition 4 and 5) results in a 2-3 dB increase in backscatter for the balsam poplar, however, this change is modulated by a parallel change in leaf moisture in the spruce. There is a large change in backscatter between conditions 11 and 12 when the ground conditions are changed from flooded to frozen and the leaves fall. The difference between condition 8 and 9 shows the change due to the balsam poplar leaves drying; this change results in little backscatter change at CVV.

In summary, for the states of interest to CO_2 flux modeling, CVV provides information on canopy freeze/thaw and soil freeze/thaw but does not show sensitivity to leaf on/off.

2) JERS-1 and RADARSAT Parameters: The above simulations were repeated using radar parameters for JERS-1 and Canada's RADARSAT. JERS-1 is an L-band, HH polarized system with an incidence angle of 35° and was launched in February 1992. RADARSAT is a C-band system with HH polarization and a capability of operating at a variety of incidence angles; 23° and 35° angles were used in these simulations; RADARSAT is scheduled for a 1994/5 launch and a 5-year mission lifetime. The results of the JERS-1 and RADARSAT simulations are shown in Table VII and Fig. 9(b)- (d).

TABLE VI
PROPERTIES USED IN SEASONAL SIMULATIONS

Property	Assumption
Dry soil temperature	5 C
Wet soil temperature	5 C
Soil volumetric moisture: dry*	0.1
Soil volumetric moisture: wet	0.3
Leaf gravimetric moisture: high	0.8
Leaf gravimetric moisture: normal	0.6
Leaf gravimetric moisture: dry	0.2
P-band snow dielectric constant	same as L-band
P-band woody dielectric constant	same as L-band
Dry and stressed woody vegetation dielectrics	same as frozen dielectrics
Ground surface roughness	small perturbation model at L-band physical optics model at C-band

* units are fractional moisture content

For both the JERS-1 and the RADARSAT parameters, there is significant change in backscatter over the season. As was shown with the AIRSAR data, the L-band shows a significant rise in backscatter with thawing (condition 1 -2) for all three forest types. The CHH RADARSAT parameters show little change due to freeze/thaw except for the white spruce which shows a drop similar to that observed with the ERS-1 CVV parameters. Soil thaw (4-5) results in little change for white spruce at LHH or CHH, but a significant rise for balsam poplar and white spruce. Leaf-on (5 6) results in a large drop in backscatter at CHH. Fall drying of the leaves (8-9) likewise results in a rise in backscatter at CHH.

3) Summary: The above modeling results show that at least two different radar channels are required to estimate growing season length. Soil freeze/thaw may be estimated with ERS-1 CVV or JERS-1 LHH channels; however, neither provide adequate sensitivity to leaf on/off. RADARSAT CHH should provide sensitivity to leaf on/off but little sensitivity to freeze/thaw for the black spruce and balsam poplar forest types. A combination of LHH and CHH or CVV and CHH should provide adequate information for estimating the key seasonal transitions.

TABLE VII
RESULTS OF MIMICS SIMULATION MODELING: ERS-1, JERS-1, AND RADARSAT MODES
(ALL VALUES ARE IN DECIBELS)

Cond	ERS-1 CVV, 23°			JERS-1 LHH, 35°			RADARSAT CHH, 23°			RADARSAT CHH, 35°		
	BP	WS	BS	BP	WS	BS	BP	WS	BS	BP	WS	BS
1	-16.43	-8.35	-13.96	**-1466**	**-12 15**	-16.83	-13.69	-7.60	-10.02	-12.73	-8 63	-11.07
2	-18.54	-12.18	**-1705**	**-12 26**	-7 25	1 1.00	-15 15	-11.95	-10.24	-13.89	-13.27	-9.33
3	-14.64	-8.49	-8.21	-3.92	-5.43	**.549**	-5 73	-5.44	.69	-5.65	**685**	-1.62
4	-14.64	-7.91	**-793**	-3.92	-5.08	-5.42	-5 73	-4.39	1.01	-5.65	-5.74	**-1 27**
5	-11.72	-9.73	**-905**	-.96	**4.19**	**-1 15**	-2 35	-5.37	2.79	-2.66	-6.78	**290**
6	-12 78	-9.73	-9.05	**-2 33**	-4 19	-1 15	-7.49	-5.37	2.79	-8.23	**-678**	**290**
7	-13.60	**.973**	-9.05	-1.93	-4 19	-1.15	-5.91	-5.37	2.79	-6.59	**-6 7x**	**290**
8	-12 63	**-11 10**	-12.24	**-4, 34**	-5.90	-4.87	-4.62	-7.99	-.69	-5.42	**.9 19**	**-0'25**
9	**-1297**	-8.50	-8 29	-3.55	**-618**	**.637**	-1.66	-5.48	.60	-2.15	-6 88	**1 70**
10	-12.97	**-7.92**	-8.02	-3.55	-5.83	-6.29	-1.66	-4.44	.92	-2 15	**5 7***	-1 35
11	-12.36	-8 19	-6.50	**.26**	**-2 83**	1.01	-3.58	-3.23	5.28	-4.60	**4 88**	**5 12**
12	-14.64	**-11 OK**	-12 16	-3.92	**.5,60**	**-4.07**	-5.73	-7.93	-.60	-5.65	9 13	-0 16
13	**-1248**	**.7,91**	**.7.93**	-2.43	-5.08	**.5.42**	-1.03	-4.39	1.01	-1.47	5 74	**-1 27**
Rnge	6.82	4.27	10.55	14,92	9,32	17.84	14.12	8.72	15.52	12.42	8.39	16.19

V. CLASSIFICATION OF FOREST TYPES

In this section we discuss the use of SAR data for classifying the landscape into units of different carbon flux. A maximum *a posteriori* polarimetric Bayes' classifier [27] was used to classify the AIRSAR data into groups corresponding to different terrain cover. Fig. 10(a) shows the results using the March 13 AIRSAR data as input, and Fig. 10(b) shows the results using the March 19 data. The classes are: clear-cat areas (CC), alder stands (AL), balsam poplar stands (BP), white spruce stands (WS), black spruce stands (BS), and river (R). Training areas representative of each forest class are the measured stands shown in Table 11. The average polarimetric characteristics of all the pixels contained in the training areas of a particular class define the polarimetric characteristics of that class, and serve as an input to the polarimetric classifier.

Classification accuracy is then computed based on the class labeling of the pixels belonging to the 12 test stands. Classification accuracy is recorded in confusion matrices, as shown in Table VIII. Vertical columns indicate how, for a particular class, various pixels are misclassified. Each vertical column totals 1 00%, and components of each vertical column denote the percent misclassification (as other classes) relative to the correct classification based on the training sites. The total classification accuracy at one frequency is computed from the average of the diagonal elements of the corresponding confusion matrix.

The results obtained on March 13 using fully polarimetric L-band data yield a total classification accuracy of 76%. WS, BP, and Al. are confused because they have similar backscatter characteristics. The results on March 19 indicate a decrease in total classification accuracy of 15% at L-band. BS is confused with CC; and the confusion between BP and WS increases.

In summary, these results indicate that thawed conditions are better than frozen conditions for mapping forest type in the BCEF floodplain forests. However, the classification accuracy is only computed on a set of test stands, i.e., dots not include all the pixels of the scene. Further testing using data corresponding to different seasons will be examined in follow-up papers to more completely assess the potential of the radar to separate various forest types and terrain covers with a high accuracy.

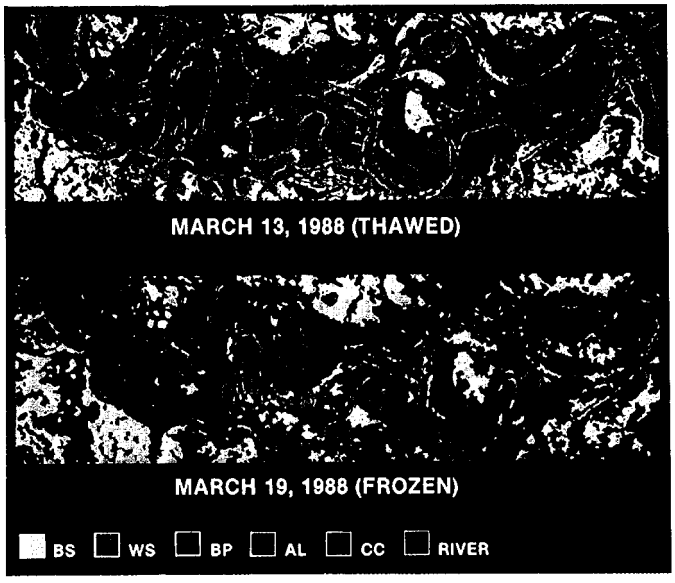

Fig. 10. Species classification maps using AIRSAR L-band fully polarimetric data for March 13 (a) and March 19 (b).

TABLE VIII
CONFUSION MATRICES FOR CLASSIFICATIONS USING POLARIMETRIC L-BAND AIRSAR DATA

March 13

Species	CC	Al.	BP	WS	BS	R
CC	7 U	3	1	O	?	2
Al.	1	70	19	13	26	o
BP	o	7	61	8	1	o
WS	1	10	17	*/h	2	0
BS	19	10	2	1	69	0
R	1	0	0	o	0	98

Accuracy = 76%

March 19

Species	CC	Al	BP	WS	BS	R
CC	7	3	4	3	0	1 9 ?
AL	1	44	18	11	4	0
0P	1	0	38	28	o	0
WS	2	3	38	53	17	0
BS	23	9	3	8	59	0
R	o	40	o	0	0	98

Accuracy = 61%

V]. Discussion

Wc have demonstrated the usc of SAR for mapping forest type or functional group for the major floodplain successional stages in interior Alaska using L-band polarimetric SAR data to an accuracy of approximately 76%. Our results also indicate the annual freeze-thaw processes of the major floodplain forest types can be observed in SAR data with a signal at L-band of 5-7 dB. Microwave model simulations show a clear sensitivity to soil freeze/thaw and leaf on/off. Given these capabilities, the application of SAR to improving annual CO_2 flux estimates in the boreal forests will be assessed. Wc first introduce an ecophysiological model developed by Bonan which uscs standard meteorological data as input to simulate daily CO_2 flux. We then combine this model with parameters which can be estimated with SAR to demonstrate how the SAR data can be used to improve annual CO_2 flux estimates.

A. *Ecophysiological Model*

Our current understanding of the ecology of boreal forests indicates that interactions among climate, soil temperature, permafrost, soil moisture, the forest floor, litter quality, and nutrient availability control stand productivity and organic matter decomposition [4], [5], [9], [35]–[38]. Bonan [7] has developed an ecophysiological model of seasonal carbon uptake and release by boreal forest ecosystems that quantifies this relationship. The model simulates daily tree photosynthesis and respiration, moss photosynthesis and respiration, and microbial respiration. Tree photosynthesis is a function of the CO_2 diffusion gradient, bulk boundary layer resistance, stomatal resistance, and mesophyll resistance. Stomatal resistance is a functinn of irradiance, foliage temperature, vapor pressure deficit, and foliage water potent ial. Tree respiration is partitioned into maintenance and growth respiration. Maintenance respiration is an exponential function of foliage temperature; growth respiration is a function of the efficiency with which new tissue is synthesized.

Bonan [6] describes the calculation of the required biophysical parameters such as stomata] resistance, foliage temperature, soil temperature, anti soil moisture. The surface energy budgets for the upper forest canopy, lower forest canopy, and ground surface arc each written in terms of the temperatures of the upper and lower canopy and the ground surface. These three equations arc solved simultaneously for the three unknown temperatures; and with ground surface temperature, evapotranspiration, and snow melt known, soil temperature and soil moisture in a multilayer soil are updated. Required meteorological parameters (air temperature, precipitation, air pressure, relative humidity, wind speed, and cloudiness) for Fairbanks were obtained based on the National Oceanic and Atmospheric Administration's (NOAA's) "typical meteorological year" as described by Bonan [6], [7].

Simulated seasonal cycles of snow depth, soil temperature, stomatal resistance, and ecosystem CO_2 flux using Bonan's model are shown in Fig. 11 for representative balsam poplar, white spruce, and black spruce stands growing on the Tanana floodplains and average climatic conditions. Viereck *et al.* [40], [41] and Van Cleve *et al.* [37], [38] describe the structure of these particular stands. The balsam poplar stand is a highly productive 60-year-old stand growing on wat m, well-drained nutrient-rich soil. The black spruce stand is an unproductive 130-year-old stand growing on cold, poorly drained, nutrient-poor soil. The white spruce stand is a productive 1 IS-year-old stand with a thick forest floor growing on well-drainccl soil.

In all stands in the simulations, snow began to accumulate in nliC1-October. The open-c:inopy black spruce and the deciduous balsam poplar stands accumulated more snow than the closed-canopy white spruce stand. Spring snow melt began in mid-April and was completed by the end of April for all stands. Soils cooled during the winter and began to warm in spring as air temperature increased and snow melted. The warmest summer soil temperatures occurred in the balsam poplar and white spruce stands. The black spruce stand had the coldest summer soil temperatures and the shortest period in which the soil was unfrozen. The seasonal changes in soil and air temperatures were reflected in the seasonal dynamics of stomatal resistance. Stomata were closed (i .c. , high resistance) during the winter months w hen air temperatures were cold and the soil was frozen. As the air warmed and the soil thawed, the stomata opened, and resistance to water vapor 10ss and CO_2 uptake decreased. 'This opening of stomata occurred approximately three weeks later in the cold black spruce stand than in the other stands, resulting in a shorter growing season. The seasonal dynamics of ecosystem CO_2 flux parallels these site conditions. During the winter months, 0-5 g CO_2 m $^{-2}$ day $^{-1}$ were lost due to respiration. In the spring, as the soil and air warmed, trees began to grow and the ecosystems absorbed significant amounts of CO_2. This uptake was greatest for the productive balsam poplar stand and least for the unproductive black spruce stand. In the fall, as the soil and air cooled, tree growth stopped and the ecosystems no longer absorbed CO_2.

The onset of CO_2 uptake in balsam poplar is driven by bud break in the spring which in turn is driven by air temperature. For white spruce and black spruce, onset of CO_2 uptake is determined by the thawing of the trees and soil which is also driven by air temperature.

Bonan's ecophysiological model can bc used with meteorological data as the only input to derive annual carbon influx as was shown in Fig. 11. These seasonal carbon cycles show that the primary drivers for estimating net annual CO_2 flux are growing season length (an early thaw or leaf-out of four weeks may change high latitude growing season length by up to 30%), maximum productivity (which decreases with season), and daily fluctuations from maximum productivity (Fig. 12). Spatial and temporal estimates of forest freeze-thaw and leaf on/off derived from SAR data can be used to obtain direct estimates of grow-

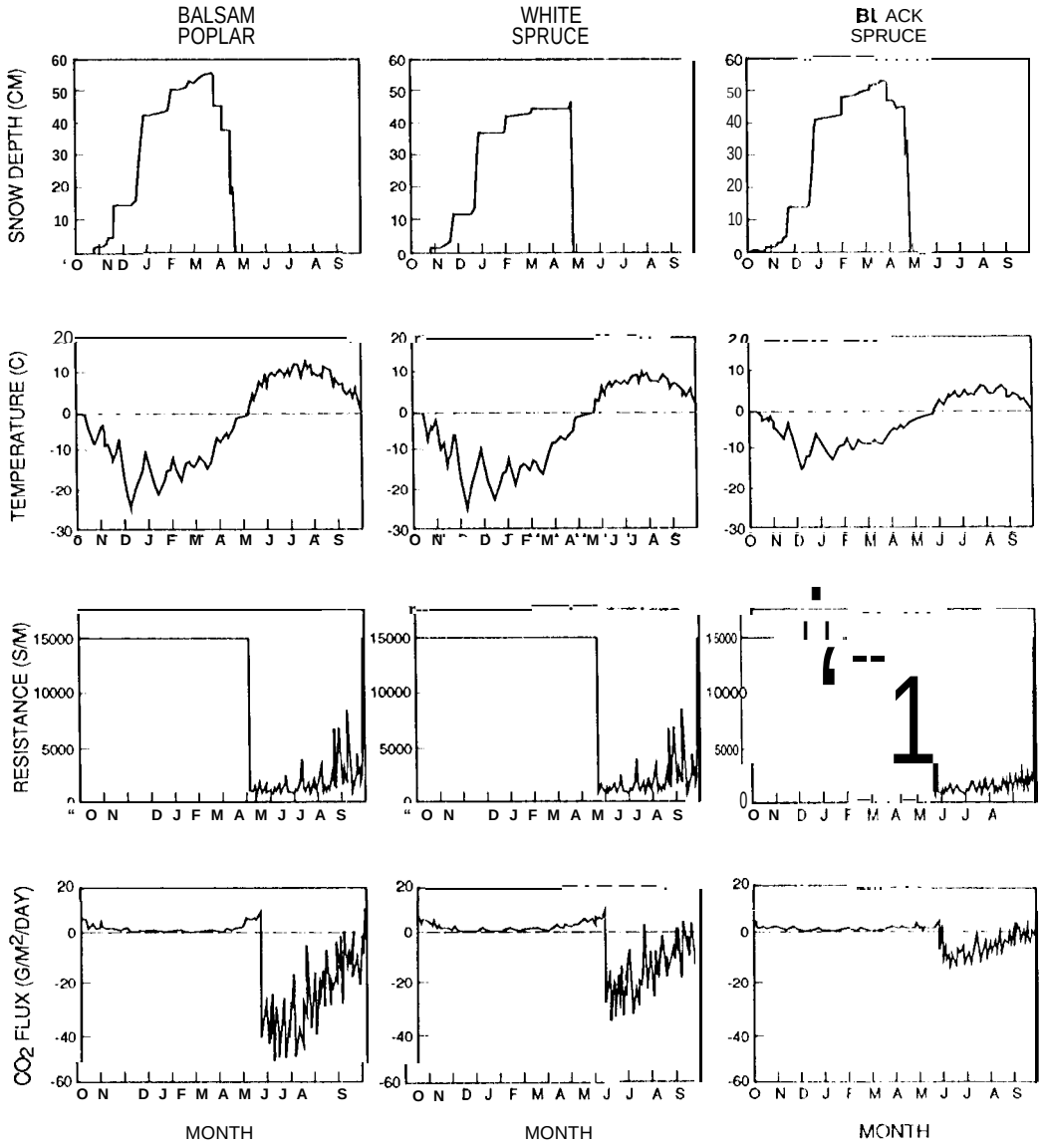

Fig. 11. Simulated daily snow depth, soil temperature, stomatal resistance, and C O_2 flux for one year from October 1 to September 30 for mature balsam poplar, white spruce, and black spruce stands growing on floodplains near Fairbanks using Bonan's ecophysiological model

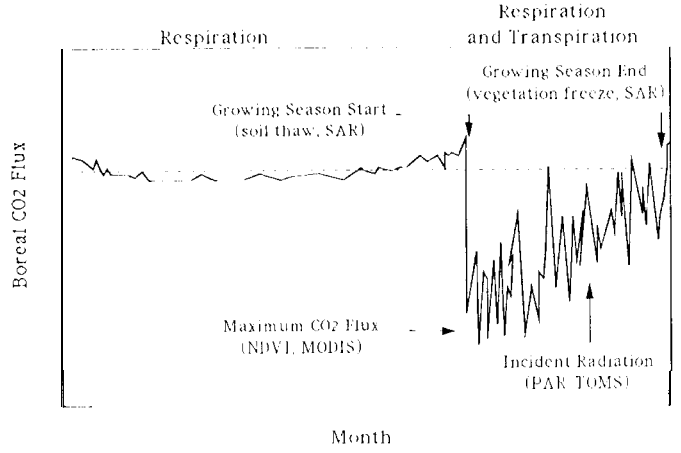

Fig. 12. Simulated CO_2 flux for while spruce indicating role of various remote sensors in determining important parameters in estimating the annual CO_2 flux.

ing season length. Productivity is related to APAR, which in turn can be derived from optical remote sensing data such as Landsat and (eventually) MODIS. Daily fluctuations in incoming radiation can be derived from a cloud sensor such as TOMS or AVHRR. Alternately, remotely sensed areal estimates of forest types (e. g., black spruce, deciduous, etc.) can be combined with Bonan's ecophysiological model output to scale stand-level CO_2 to landscape-average fluxes.

Here we use a combination of SAR- and mmlcl-derived parameters to investigate the variability in landscape CO_2 flux with seasonal state.

B. CO_2 Flux Maps

Fig. 13 shows the model diagram from which CO_2 flux maps and scclle-averaged CO_2 flux for the seasonal states captured by AIRSAR are derived using a combination of

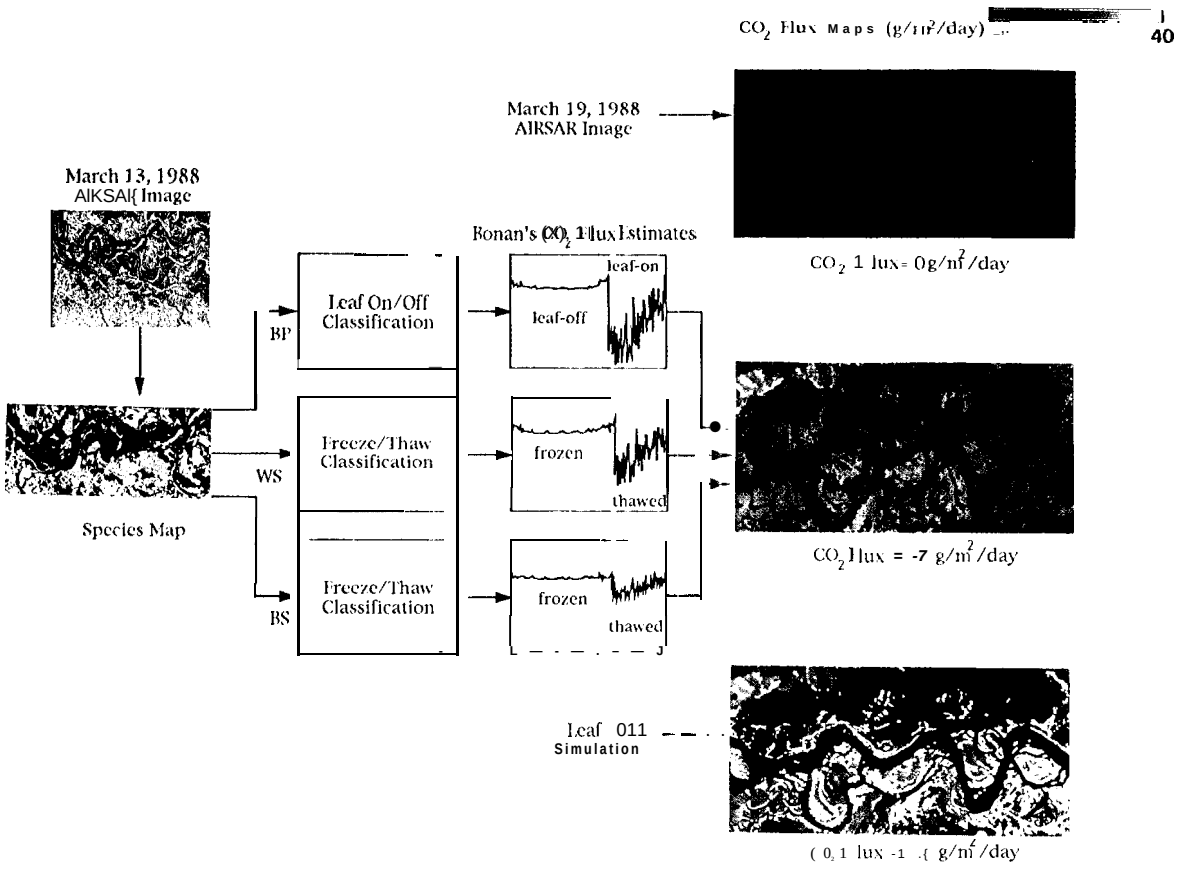

Fig. 13. Potential CO_2 flux algorithm for which SAR data are used in species classification and seasonal state monitoring, and Bonan's model is used for seasonal CO_2 flux amplitude estimates. The March 13 and 19 data were used as input to derive the first two CO_2 flux maps. Leaf-on was simulated for the third map. Scene-averaged CO_2 flux estimates are shown for each map.

SAR data and ecophysiological model output. Forest type maps are first generated using the March 13 AIRSAR data. For the two spruce forest types, the seasonal state is determined using the backscatter ranges from equations (1)-(4). For the thawed spruce, the CO_2 flux derived by Bonan (Fig. 11) are then applied. For frozen spruce and leafless poplars, the CO_2 flux is 0. Thawed white spruce and black spruce have average daily CO_2 fluxes of 22 and -10 g $m^{-2}day^{-1}$, respectively. These daily CO_2 fluxes are then displayed as a CO_2 flux map and the average scene CO_2 flux is derived. To further illustrate the value of monitoring the leaf on/off conditions, we simulate the addition of balsam poplar leaves to the March 13 scene to obtain a state when both the spruce and the poplars are exchanging CO_2. The result is also shown in Fig. 13 using an average daily CO_2 flux for balsam poplar of -35 g $m^{-2}day^{-1}$. From the frozen to the thawed to the leaf-on state, the scene CO_2 flux changes from 0 to -7 to 13 g $m^{-2}day^{-1}$. Such a model must be validated for many more forest types and seasonal conditions; however, these results illustrate the importance of both landscape classification and seasonal state to any estimate of landscape CO_2 flux.

C. Improvement with Classification

Bonan's ecophysiological model [6], [7] requires forest type coverage percent to derive landscape CO_2 flux estimates. The percent areal extents of BS, WS, BP, AL, CC, and R were estimated using the classified AIRSAR scene (incidence angle range from 37.5° to 52.5°) from March 13 [Fig. 10(a)]; the scene contains 16.0% CC, 17.5% AL, 13.0% BP, 22.2% WS, 18.0% BS, and 13.3% R (Table IX). The annual CO_2 flux for each of these landscape types was then simulated using Bonan's ecophysiological model [7]. Table IX shows the tree, moss, microbe, and total ecosystem CO_2 fluxes, where a negative flux indicates CO_2 uptake. The fluxes for black spruce are the average of nine stands, and the fluxes for white spruce and balsam poplar are the average of five white spruce and three balsam poplar stands, respectively. The river had no CO_2 flux. The area classified as clearcut has no trees, therefore no CO_2 flux was assumed for this estimation. No data exist for alder; here we assume fluxes equivalent to aspen [7]. The total landscape CO_2 influx was estimated to be 987 g CO $m^{-2}yr^{-1}$.

TABLE IX
LANDSCAPE ESTIMATES OF ANNUAL CO_2 FLUXES[a]

Stand	Area (%)	Net Photosynthesis (g $CO_2/m^2/yr$) Tree	Moss	Microbe	Ecosystem
AL***	17.5	-2123	0	298	-1825
BP	13.0	-3195	0	514	-2681
WS	22.2	-1212	-216	322	-1106
us	18.0	-354	-200	171	-384
CC	16.0	0	-200	171	-29
RIVER	13.3	0	0	0	0
Landscape	100.0				-987

[a] Negative fluxes indicate CO_2 uptake; simulated annual CO_2 flux data from Bonan (1991b)
[b] Based on March 13 AIRSAR data
[c] No data exits for alder; assumed CO_2 flux equivalent to aspen (Bonan 1991 b).

The landscape CO_2 flux derived from the model is sensitive to forest type. For example, if all forests in this area (i.e., 70.7 % of the scene) were balsam poplar, the model estimate of the landscape CO_2 influx would have been 1900 g CO_2 $m^{-2}yr^{-1}$, or more than a factor of two greater than the above estimate. If all forests were BS, the estimated CO_2 influx would be 276 g CO_2 $m^{-2}yr^{-1}$, or about one-quarter of the estimate based on the actual forest type distribution. If the entire scene were BP, WS, or BS (i. e., without river or clearcut areas), the CO_2 influx would be 2681 (nearly three times greater), 1106 and 384 (about one-third) g CO_2 $m^{-2}yr^{-1}$, respectively. The differences, in CO_2 influx predicted by the model for three forest types are due to differences among the types in both photosynthetic rates per unit of leaf area and total leaf area. These simulations demonstrate the importance of accurately determining the spatial mix of forests by CO_2 functional group or forest type.

VII. Summary

This paper demonstrates using AIRSAR data and MIMICS model simulations so that it is possible to both monitor seasonal change and map forest type using multitemporal spaceborne SAR data in level terrains. The importance of SAR-derived estimates of seasonal state and forest type or functional group as input to the ecophysiological models was demonstrated. other sensors, such as Landsat and AVHRR, may offer similar abilities for landscape classification and monitoring leaf on/off periods. We believe SAR is unique in its ability to monitor freeze/thaw duration.

With the launch of ERS- 1 in the summer of 1991 followed by ERS-2, JERS-1, and RADARSAT, the opportunity to begin long-term monitoring of these parameters should allow important advances in our understanding of the role of the boreal forests in the global carbon cycle. Additional studies, particularly for upland forests, are necessary to fully understand our ability to use SAR on a regional basis to monitor growing season length and map forest type in boreal forests. Outstanding ecological questions include understanding the process of soil and canopy freezing and thawing relative to start and stop of transpiration. Outstanding SAR remote sensing questions include validating our ability to monitor leaf on/off and soil freeze/thaw independent of canopy freeze- thaw. The microwave models indicate that it is possible to observe these processes; however, remote sensing data are required for validation.

Acknowledgments

The authors acknowledge the work of many people who participated in the ground truth data collection including C. Slaughter, B. Wood, A. Davis, B. Jaeger, and P. Adams of the Institute of Northern Forestry. At the Jet Propulsion Laboratory, the contributions of J. Holt and 'T. Freeman were invaluable in the data organization and calibration. The ideas for using classification algorithms similar to those used in the Alaska SAR Facility (ASF) Ice Geophysical Processor ((il'S) were developed based on discussions with B. Holt. We would also like to acknowledge the contributions of and discussions with the International Forest Investigations Team (IFIT), particularly F. Ulaby, E. Kasischke, N. Christensen, and D. Simonett. The contributions of R. Zimmermann in the analysis of the canopy data were also extremely valuable. Finally, we would like to thank R. Waring for his extensive reviews of this work.

References

[1] R. B. Bacastow, C. D. Keeling, and T. P. Whorf, "Seasonal amplitude increase in atmospheric CO_2 concentration at Mauna Loa, Hawaii, 1959 1982," *J. Geophys. Res.*, vol. 90, pp. 10529- 10540, 19X5.

[2] G. B. Bonan, "A computer model of the solar radiation, soil moisture, and soil thermal regimes in boreal forests," *Ecol. Model.*, vol. 45, pp. 2.75 306, 1989.

[3] "Environmental factors and ecological processes controlling vegetation patterns in boreal forests," *Landscape Ecol.*, vol 3, pp. 111-130, 1989.

[4] , "Carbon and nitrogen cycling in North American boreal forests. 1. Litter quality and soil thermal effects in interior Alaska," *Biogeo-*[/1('/)1., vol. I 0, pp. 1-28,1990.

[5] , "Carbon and nitrogen cycling in North American boreal forests. II, Biogeographic patterns," *Can. J. Forest Res.*, vol. 20, pp. 1077-1088, 1990.

[6] 'CA biophysical surface energy budget analysis of soil temperature in the boreal forests of interior Alaska," *Water Resour.* t/(\., vol. 27, pp. "67-781, 1991.

[7] "Atmosphere- biosphere exchange of carbon dioxide in boreal forests," *J. Geophys. Res.*, vol. **96,** pp. 7301-7312, 1991.

[8] , "Seasonal and annual carbon fluxes in a boreal forest landscape," *J. Geophys Res.*, vol. **96,** pp. 17329-17338, 1991.

[9] G. B. Bonan and H. H. Shugart, "Environmental factors and ecological processes in boreal forests," *Ann. Rev. Ecol. Syst.* 20, 1-28.

[10] G. B. Bonan and M. D. Korzuhin, "Simulation nf" moss and tree dynamics in the boreal forests of interior Alaska," *Vegetatio*, vol. 84, pp. 31-41, 1989.

[11] G. B. Bonan H. H. Shugart, and D. L. Urban, "The sensitivity of some high-latitude boreal forests to climatic parameters," *Climatic Change*, vol 16, pp. 9-29, 1990.

[12] R. D'Arrigo, G. C. Jacoby, and I. Y. Fung, "Boreal forests and atmosphere biosphere exchange of carbon dioxide," *Nature*, vol. 329, pp. 321-323. 1987.

[13] M. C. Dobson, K. C. McDonald, and F. T. Ulaby, "Modeling of forest canopies and analysis of polarimetric SAR data," Radiation Lab. Tech Rep. 020143 -1-1." Univ. Michigan Radiation Lab., Dec. 1989.

[14] M. C. Dobson, K. [. McDonald, F. T. Ulaby, and J. B. Way, "Effects of temperature on radar backscatter for boreal forests," in *Int. Geosci. Remote Sensing Soc. Conf.*, 1[;AA'L!!% '90, I 990

[15] M. J. Foote, "Classification, description, and dynamics of plant communities after fire in the taiga of interior Alaska," Res. Paper PNW-307, Portland, OR, U. S. Dep. Agriculture, Forest Service, Pacific Northwest Forest and Range Experiment Station. 108p.

[16] R. H. Gammon, E. '1'. Sundquist, and P. J. Fraser, "History of carbon dioxide in the atmosphere, 27- 62, " in *Atmospheric Carbon Dioxide and the Global Carbon Cycle*, Rep. DOE/ER-0239, J. R. Trabalka, Ed., U. S. Dep. Energy, Carbon Dioxide Res., 1985.

[17] D. Gates, "Water relations of forest trees, " *IEEE* 71(111,<.*Geosci. Remote Sensing*, vol. 29, pp. 836 842, 1991

[18] R. A. Houghton, "Biotic changes consistent with the increased seasonal amplitude of atmospheric CO_2 concentration," J. *Geophys. Res.*, vol. 92, pp. 4223-4230, 1987.

[19] R. A. Houghton, R. D. Boone, J. M. Melillo, C. A. Palm, G. M. Woodwell, N. Myers, B. Moore, and 1). L. Skole, "Net flux of carbon dioxide from tropical forests in 19x(), " *Nature*, vol. 316, pp. 617- 620, 1985.

[20] B. Jaeger, Report on stand characteristics measured in Bonanza Creek Experimental Forest for the SAR-IFIT Project, Forest Soils lab., Univ. Alaska, Fairbanks, Dec. 1988.

[21] R. Kwok, E. Rignot, J. B. Way, A. Freeman, and J. Holt, "Polarization signatures of frozen and thawed forests of varying environmental state," *IEEE Trans.* Gee).s(i. *Remote Sensing*, this issue.

[22 1). A. Lashof, "The dynamic greenhouse: Feedback processes that may influence future concentrations of atmospheric trace gases and climatic change," *Climatic Change*, vol. 14, pp. 213242, 1989.

[23 G. H. Manning, M. R. C. Massie, and J. Rudd, "Metric single-trt.c weight table for the Yukon Territory," Inform. Rep. 11X-X-250, Canadian Forestry Service, Pacific Forest Research Centre, Victoria, B.C., 60 p.

[24 K. C. McDonald, M. [. Dobson, and F. T. Ulaby, "Using MIMICS to model L-band multi-angle and multi-temporal backscatter from a walnut orchard," *IE*<1,"*Trans. Geosci. Remote Sensing*, vol. 28, pp. 477.491, 1990.

[25] — "Modeling multi-frequency diurnal backscatter from a walnut orchard," *IEEE Trans. Geosci. Remote Sensing*, vol. 29. pp. 852-863, 1991.

[26] W. M Post, "Repot-(of a workshop on climate feedbacks and the role of peatlands, tundra, and boreal ecosystems in the global carbon Cycle, " Tech. Man. ORNL/TM-11457. Oak Ridge Nat. Lab., Oak Ridge, TN, 1990.

[27] E. Rignot and R. Chellappa, "Segmentation 01 polarimetric synthetic aperture radar data, " *IEEE Trans. Signal Processing*, vol. 1, pp. 281 300, 1992,

[28] J. E. Roth and A. M. Davis, "Stand characteristics of Bonanza Creek Experimental Forest, Alaska, 1990 summer field measurements," Rep. inst. Northern Forestry, USDA Forest Set\Vice, Fairbanks, AK, Dec. 1990.

[29] M. E. Schlesinger and J. F. B. Mitchell, "Climate model simulations of the equilibrium climatic response to increased carbon dioxide," *Rev. Geophys.*, vol. 25, pp. 760- 798, 1987.

[30] 'f. Singh, "Weight tables for important tree species in the Northwest Territories," Forest Manage. Note 27, Canadian Forest Service, Northern Forest Research Centre, Edmonton, Aln, 4 p. plus tables, 1983.

[31] P. Y. Tans, 1. Y. Fung, and "1'. Takahashi, "Observational constraints on the global atmospheric CO_2 budget," *Science*, vol. 247, pp. 1431-1438, 1990.

[32] F. '1'. Ulaby and C. Elachi, Eds., *Radar Polarimetry for Geoscience Application*. Dedham, MA: Artech House, 1990.

[33] F. 1'. Ulaby, K. Sarabandi, K. McDonald, M. Whitt, and M. C. Dobson, "Michigan Microwave Canopy Scattering Model, " *Int. J. Remote Sensing*, vol. 11, pp. 12231254, 1990.

[34] K. Van Cleve, F. S. Chapin, III, C. 'f. Dyrness, and L. A. Viereck, "Element cycling in taiga forests: State-factor control," *BioScience*, vol. 41, pp. 7888, 1991.

[35] K. Van Cleve and J. Yarie, "Interaction of temperature, moisture, and soil chemistry in controlling nutrient cycling and ecosystem development in the taiga of Alaska," in *Forest Ecosystems in the Alaskan Taiga*, K. Van Cleve, F. S. Chapin, P. W. Flanagan, L. A. Viereck, and C. T. Dyrness, Eds. New York: Springer-Verlag, 1986, pp. 160-189.

[36] K. Van Cleve and L. A. Viereck, "Forest succession in relation to nutrient cycling in the boreal forest of Alaska," in *Forest Succession: Concepts and Applications*, D. West, H. Shugart, and D. Botkin, Eds. New York: Springer Verlag Advanced Texts in Life Sciences, 1981, pp. 185 211.

[37] K. Van Cleve, C. T. Dyrness, 1 A. Viereck, J. Fox, F. S. Chapin, and w. Oechel, "Taiga ecosystems in interior Alaska," *Bioscience*, vol. 33. pp. 39-44, 1983.

[38] K. Van Cleve, L. Oliver, R. Schlentner, L. A. Viereck, and C. '1'. Dyrness, "Productivity and nutrient cycling in taiga forest ecosystems," *Can. J. For est Res.* vol. 13, pp. 747-706. 1983.

[39] J. van Zyl, "Unsupervised classification of scattering mechanism using radar polarimetry ." *IEEE Trans. Geosci. Remote Sensing*, vol. 27, pp. 36-45, 1989.

[40] L. A. Viereck, ('. T Dyrness, K. Van Cleve, and M. J. Foote, "Vegetation, soils, and forest productivity in selected forest types in interior Alaska," *Can. J. Forest Res.*, vol. 13, pp. 703720, 1983.

[41] "Productivity and nutrient cycling in taiga forest ecosystems," *Can. J Forest Res.*, vol. 13, pp. 747 766, 1983.

[42] J. B. Way, ,1. Paris, E Kasischke, C. Slaughter, L. Viereck, N. Christensen, hf. (. Dobson, 1. '1 Ulaby, J. Richards, A. Milne, A. Sieber, F. J. Ahern, D. Simonett, R. Hofler, M. Imhoff, and J. Weber, "The effect of changing environmental conditions on microwave signatures of forest ecosystems: Preliminary results of the March 1988 Alaska aircraft SAR experiment," *Int. J. Remote Sensing*, vol 11, pp. 1119- 1144, 1990.

[43] J. B. Way, J. Paris, M. C Dobson, K. McDonald, F. '1 Ulaby, J. A. Weber, S. L Ustin, V. C. Vanderbilt, and E. S. Kasischke, "Diurnal change in trees as observed by optical and microwave sensors: '1 he EOS synergism study ," [[. [1.' *Trans. Geosci. Remote Sensing*, vol. 29, pp. 807 821, 1991.

[44] J. B. Way and I A. Smith, "The evolution of synthetic aperture radar systems and their progression to the EOS SAR," *IEEE Trans. Geosci Remote Sensing*, vol. 29, pp. 962-985, 1991.

[45] J. B. Way, K. McDonald, I Paylor, (i. Karas, S. Chernobieff, and N. Biery, "Collected data of the Bonanza Creek Experimental Forest, Volumes I and II, Version 1," CD Rom, Jet Propulsion Lab., Pasadena, (A, 1992.

[46] J. A. Weber and S. L. Ustin, "Diurnal water relations of walnut trees: Implications for remote sensing," *IEEE Trans. Geosci. Remote Sensing*, vol. 29, pp. 854874, 1990.

[47] J. Yarie and K. Van Cleve, "Biomass and productivity of white spruce stands in interior Alaska " *Can. J. Forest Res.*, vol. 13, pp. 767-772. 1983.

JoBea Way (M'86) was born in Lorraine, OH in 1954. She received the B. S. degree in chemistry from the University of California, Berkeley, and the M.S. and Ph.D. degrees in planetary sciences from the California Institute of Technology.

She has worked at the Jet Propulsion Laboratory since 1976. She is the Principal Investigator of an ERS-1 Forest Project to determine the effects of canopy temporal variations on radar backscatter. Her research is based in Alaska at the Bonanza Creek Experimental Forest. She is a Team Member on the EOS SAR Facility Instrument Team and Co-Investigator with Dr. Robert Dickinson on an EOS Interdisciplinary Investigation to study global climate change. She was recently selected as a Principal Investigator for the NASA BOREAS Project to utilize SAR-derived measurement of seasonal state in carbon flux models. She has been involved in all of JPL's spaceborne SAR projects since 1981. She was the Science Coordinator for the first Shuttle Imaging Radar, SIR-A, and the Experiment Scientist for its follow-on, SIR-B. She is currently coordinating the vegetation studies for SIR-C/X-SAR and will be one of the payload communicators with the astronauts during the mission.

Eric J. M. Rignot (M'91) was born in Chambon sur Lignon, France. He received the Engineer's diploma from the Ecole Centrale des Arts et Manufactures Paris in 1985, the M.S. degree in astronomy from the University of Paris VI in 1986, and M.S.'s in aerospace engineering and in electrical engineering in 1987 and 1988, respectively, and the Ph.D. in electrical engineering from the University of Southern California in 1991.

He was employed as a Research Assistant at the University of Southern California in the Department of Aerospace Engineering in 1986–1988. He then joined the Radar Science and Engineering Section at the Jet Propulsion Laboratory, California Institute of Technology. He is a Principal Investigator on the Greenland AIRSAR Experiment, and a Co-Investigator on an ERS-1 SAR project and BOREAS. His current research interests include analysis of radar scattering from glacier facies, monitoring of environmental conditions in boreal forests using ERS-1 and J-ERS-1 SAR, and retrieval of forest parameters from polarimetric SAR data.

Dr. Rignot is a member of AGU.

Kyle C. McDonald (S'89–M'91) was born in Columbus, OH, on October 23, 1960. He received the Bachelor of Electrical Engineering degree (cooperative plan with highest honors) from the Georgia Institute of Technology, Atlanta, in 1983; the M. S. degree in *numerical science* from Johns Hopkins University, Baltimore, MD, in 1985, and the M.S. and 1'11.1). degrees in electrical engineering from The University of Michigan, Ann Arbor, in 1986 and 1991, respectively.

From 1983 to 1985 he was with the Johns Hopkins University Applied Physics Laboratory where he was involved with the design and development of oceanographic sensor systems. From 1985 to 1991 he was a Graduate Student Research Assistant and NASA Fellow at The University of Michigan Radiation Laboratory where he studied problems related to modeling radar backscatter from tree canopies. In 1991 he joined the Jet Propulsion Laboratory in Pasadena, CA, where he is currently working in the Hydrology, Soils, and Ecology Group. His present research activities include interfacing radar backscatter models to biosphere–atmosphere interaction models and analysis of the temporal change characteristics observed in radar backscatter from forest ecosystems as related to hydrological and ecological processes.

Ram Oren was born in Hanot, Israel, on February 4, 1952. He studied one year in the Faculty of Mathematics and Natural Sciences, the Hebrew University, Jerusalem, and in 1979 he received the B. S. degree in forest management from Humboldt State University, Arcata, CA. He received the M.S. and Ph.D. degrees in forest ecology from Oregon State University, Corvallis, in 1981 and 1984, respectively.

In Oregon he studied the dynamics of biomass and canopy leaf area in relations to both disturbance and water availability. In Germany (1985–1986), during a postdoctoral research on the forest decline phenomena, he composed a nutritional disharmony model which explains and predicts temporal and spatial anomalies in the decline phenomena. Since 1986 he has been studying nutrient relations both at Duke University, where he is currently an Associate Professor in the School of the Environment, and in Germany. Since 1990 he has held a joint appointment with Cal. Tech's Jet Propulsion Laboratory. With colleagues at JPL he has studied vegetation water use in tropical, subtropical, temperate, and boreal forest ecosystems, as well as radar application to ecological research.

Ronald Kwok received the B. Sc. (summa cum laude) degree from Texas A&M University, College Station, in 1976, and the Ph. D. degree from Duke University, Durham, NC, in 1980. He was a Postdoctoral Fellow at the University of British Columbia, Vancouver, B.C., in 1981.

In 1985, he joined the Radar Science and Engineering Section at the Jet Propulsion Laboratory in Pasadena, CA, where he developed techniques for analysis of SAR imagery and served in a radar system engineering capacity on the Magellan and Alaska SAR Facility projects. He is currently Group Supervisor of the SAR Systems Development and Processing Group responsible for research and development of analysis and processing techniques for SAR data. His current interests include the application of remote sensing to the study of land and sea ice.

Dr. Kwok is a member of the American Geophysical Union, American Meteorological Society, Electromagnetics Academy, Tau Beta Pi, Phi Kappa Phi, and Eta Kappa Nu.

Gordon Bonan, photograph and biography not available at time of publication.

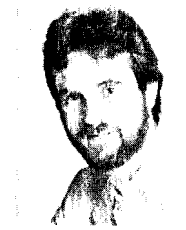

Myron Craig Dobson (M'80–SM'91) received the B.A. degrees in geology and anthropology from the University of Pennsylvania, Philadelphia, in 1973, and the M. A. degree in geography from the University of Kansas, Lawrence, in 1981.

He is an Associate Research Scientist at the University of Michigan. From 1975 to 1984 he worked at the Remote Sensing Laboratory of the University of Kansas Center for Research, Inc., where he managed several experimental programs related to microwave remote sensing of terrain. Specific research projects focused on the microwave dielectric properties of soils, microwave sensor response to soil moisture and crop canopy cover using truck-mounted and airborne scatterometers and radiometers, and multitemporal simulations of orbital SAR imagery. Since 1984 he has been with the Radiation Laboratory of the Electrical Engineering and Computer Science Department of the University of Michigan, where he conducts research on the microwave dielectric properties of vegetation and radar backscattering properties of forests.

Leslie A. Viereck was born in New Bedford, MA, on February 2(1. 1930. He received the B. A. degree in botany from Dartmouth College in 195 I; and the M. S. degree in botany and the Ph. D. degree in plant ecology from the University of Colorado in Boulder, in 1957 and 1963, respectively.

He did graduate work at the University of Alaska, McGill University, and the University of Colorado. In 1959 he joined the Faculty of the University of Alaska, Fairbanks, where he taught courses in botany and ecology and conducted eco-

logical research in northwestern Alaska related to the AEC's Project Chariot. in 1963 he joined the Staff of the USDA Forest Service's Institute of Northern Forestry as a Research Plant Ecologist. His field of research interest has been primarily in forest succession following wildfire and river deposition, as well the relationship between vegetation and permafrost. He is senior author of two major publications related to Alaska vegetation- "Trees and Shrubs of Alaska" and "The Alaska Vegetation Classification. "

Dr. Viereck received an Honorary Doctor of Science Degree in 1993 from the University of Alaska, Fairbanks, for his lifetime work on the ecology of the vegetation of Alaska.

Joanna E. Roth, photograph and biography not available at time of publication.